JOURNAL OF AGRICULTURAL AND FOOD CHEMISTRY

Article

pubs.acs.org/JAFC

Efficient Fluorescence Energy Transfer System between CdTe-Doped Silica Nanoparticles and Gold Nanoparticles for Turn-On Fluorescence Detection of Melamine

Feng Gao,* Qingqing Ye, Peng Cui, and Lu Zhang

Anhui Key Laboratory of Chemo/Biosensing, College of Chemistry and Materials Science, Anhui Normal University, Wuhu 241000, People's Republic of China

Supporting Information

ABSTRACT: We here report an efficient and enhanced fluorescence energy transfer system between confined quantum dots (QDs) by entrapping CdTe into the mesoporous silica shell (CdTe@SiO_2) as donors and gold nanoparticles (AuNPs) as acceptors. At pH 6.50, the CdTe@SiO_2−AuNPs assemblies coalesce to form larger clusters due to charge neutralization, leading to the fluorescence quenching of CdTe@SiO_2 as a result of energy transfer. As compared with the energy transfer system between unconfined CdTe and AuNPs, the maximum fluorescence quenching efficiency of the proposed system is improved by about 27.0%, and the quenching constant, K_{sv}, is increased by about 2.4-fold. The enhanced quenching effect largely turns off the fluorescence of CdTe@SiO_2 and provides an optimal "off-state" for sensitive "turn-on" assay. In the present study, upon addition of melamine, the weak fluorescence system of CdTe@SiO_2−AuNPs is enhanced due to the strong interactions between the amino group of melamine and the gold nanoparticles via covalent bond, leading to the release of AuNPs from the surfaces of CdTe@SiO_2; thus, its fluorescence is restored. A "turn-on" fluorimetric method for the detection of melamine is proposed based on the restored fluorescence of the system. Under the optimal conditions, the fluorescence enhanced efficiency shows a linear function against the melamine concentrations ranging from 7.5×10^{-9} to 3.5×10^{-7} M (i.e., 1.0−44 ppb). The analytical sensitivity is improved by about 50%, and the detection limit is decreased by 5.0-fold, as compared with the analytical results using the CdTe−AuNPs system. Moreover, the proposed method was successfully applied to the determination of melamine in real samples with excellent recoveries in the range from 97.4 to 104.1%. Such a fluorescence energy transfer system between confined QDs and AuNPs may pave a new way for designing chemo/biosensing.

KEYWORDS: *melamine, fluorescence energy transfer, raw milk, milk powder*

INTRODUCTION

Melamine (1,3,5-triazine-2,4,6-triamine), a trimer of cyanamide (CH_2N_2), is a basic heterocyclic triazine organic compound primarily used in the synthesis of melamine formaldehyde resins for the manufacturing of chemical and industrial products and medical materials.[1] Unfortunately, in recent years, melamine has been illegally adulterated in pet foods, infant formulas, and animal feeds to increase the apparent content of crude protein due to its nitrogen content as high as 66% by mass.[2] As we know, excessive intake of melamine above the safety limit (2.5 ppm in the United States and European Union, 1 ppm for infant formula in China) may result in the formation of insoluble melamine cyanurate crystals in the kidney, which finally causes renal failure and even death.[2] Consequently, the development of approaches for the detection of melamine in milk products and animal feeds has become very important to public health. Currently, a number of analytical methods including liquid/gas chromatography,[3,4] liquid/gas chromatography coupled with mass spectrometry,[5−8] gas chromatography−mass selective detection (GC-MSD),[9] mass spectrometry,[10] micellar electrokinetic chromatography,[11] capillary zone electrophoresis,[12] enzyme-linked immunosorbent assay (ELISA),[13] surface-enhanced Raman spectrometry,[14] electrochemical methods,[15,16] molecularly imprinted techniques,[17] and optical methods such as chemiluminescence,[18] colorimetric detection,[19,20] and fluorimetric methods[21,22] have been developed for the determination of melamine. However, most of these developed methods, such as chromatography-corrective methods,[3,9] mass spectrometry,[10] and ELISA[13] are generally time-consuming and also require relatively expensive instrumentation and complicated analytical procedures. Therefore, it is of considerable significance to develop sensitive, simple, and low-cost methods for the detection of melamine. Optical methods, especially fluorimetric methods, offer many advantages such as high sensitivity, simple instruments, easy operation, and the ability to measure multiple fluorescence properties. More especially, the fluorescence-based methods relying on fluorescence energy transfer (FET) techniques, which could occur when the emission spectrum of the donor and the absorption spectrum of the acceptor are appreciably overlapped to an extent, have attracted more and more attention.[23,24] As a spectroscopic technique, FET has been widely used in various research areas, especially in structural biology and analytical chemistry.[24] These distinguished abilities of the FET technique intrigue us to develop new FET systems

Received: January 30, 2012
Revised: March 25, 2012
Accepted: March 25, 2012
Published: March 26, 2012

dx.doi.org/10.1021/jf300386y | J. Agric. Food Chem. 2012, 60, 4550−4558

for the determination of melamine. To date, there are only few reports regarding the FET detection of melamine.[22]

Recently, gold nanoparticles (AuNPs) have been increasingly used in FET-based analytical applications as acceptors (quenchers). AuNPs possess high extinction coefficients (e.g., up to 8×10^8 M^{-1} cm^{-1} for 18 nm AuNPs at 520 nm) in the UV−vis regions and a broad absorption band.[25,26] These distinguished optical properties allow AuNPs to act as efficient acceptors for most fluorophores.[22,25−28] By taking advantage of the strong quenching ability of AuNPs, many efficient fluorescence sensors based on FET have been developed for the assays of biological molecules and ions.[22,25−28] On the other hand, quantum dots (QDs) are widely employed as donors in FET systems for signaling probes because of several advantages over commonly used organic fluorescent dyes, that is, tunable, narrow, and symmetric emission spectra and broad excitation spectra. They still suffer from some drawbacks such as sensitivity to oxygen and the outer environment and instability of their emission, which results in irreproducible fluorescence signals for analysis.[29,30] Fluorophore-doped silica core−shell nanoparticles (SiNPs), which use silica as the shell and fluorophores as the core, possess some distinct advantages. For example, a single nanoparticle contains a large number of fluorophores, which greatly increases the fluorescence signal as compared to one fluorophore. SiNPs can efficiently reduce the outer environmental interference with fluorophores when doped in the silica network, enabling they are antiphotobleaching and therefore have excellent photostability.[27,31−39]

On the basis of the above strategy, a novel efficient FET system between QDs, CdTe-doped silica nanoparticles (denoted as CdTe@SiO_2) as donors, and AuNPs as acceptors has been developed in this study. As shown in Scheme 1, AuNPs are noncovalently adsorbed on CdTe@SiO_2 via an electrostatic interaction, resulting in large fluorescence quenching due to FET between the CdTe@SiO_2 and the AuNPs. Upon addition of melamine, melamine molecules can interact with AuNPs via covalent binding of the amino group (NH_2−) of melamine to the surface of AuNPs, which leads to the dissociation of AuNPs from the surfaces of CdTe@SiO_2 and thus the fluorescence of CdTe@SiO_2 restore (turn-on). On the basis of the restored fluorescence, a homogeneous assay for the melamine is proposed. For comparison, the FET system between free CdTe (i.e., without doping into SiO_2) and AuNPs was also investigated for the determination of melamine, and the results showed that improved analytical performances including sensitivity and detection limit were achieved with the proposed FET system.

Scheme 1. Schematic Illustration of the Principle of "Turn-On" Fluorescence Detection of Melamine Based on Enhanced FET between CdTe@SiO_2 and Au NPs in Aqueous Solution[a]

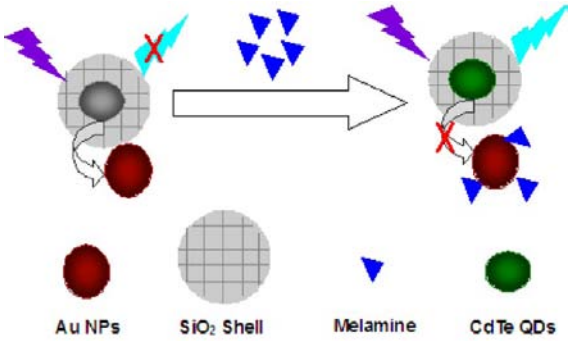

[a]The sizes of the materials are not the real scales to show the expression clearly.

MATERIALS AND METHODS

Instrumentation. The fluorescence spectra were performed using a LS-55 fluorescence spectrophotometer (PerkinElmer Co.) equipped with a quartz cell (1 cm × 1 cm). UV−vis absorption spectra were obtained with a UV-3010 spectrophotometer (Hitachi, Japan). Morphological characterization of the silica nanoparticles and AuNPs was performed with an S-4800 field emission scanning electron microscopy (SEM) (Hitachi, Japan) and Hitachi H-600 transmission electron microscopy (TEM) (Tokyo, Japan). The desired pH buffer solutions were adjusted with a pHS-3c pH meter (Shanghai, China).

Materials. Chloroauric acid tetrahydrate ($HAuCl_4 \cdot H_2O$) was purchased from Aladdin-Reagent Co. Trisodium citrate was obtained from Sinopharm Chemical Reagent Co., Ltd. (Shanghai, China). Tetraethylorthosilicate (TEOS) and ammonia solution (25%, w/w) were purchased from Sigma. Te powder (60 mesh, 99.999%) was purchased from Alfa Aesar. $NaBH_4$, $CdCl_2 \cdot 2.5H_2O$, and glutathione (reduced) were obtained from Shanghai No. 3 Chemical Co. (Shanghai, China). Melamine was provided by Aldrich (United States). The buffer solutions with desired pH were prepared by 0.01 M KH_2PO_4−Na_2HPO_4. All other reagents were of at least analytical grade and used without any further purification. Doubly deionized water was used throughout.

Synthesis of AuNPs. AuNPs were prepared by the citrate reduction of $HAuC1_4$ using the method described in our previous reports.[27,28] All glassware used in preparation of AuNPs was cleaned with freshly prepared concentrated HCl/HNO_3 mixture (3:1, v/v) and rinsed thoroughly with H_2O and finally dried before use. Typically, 99.0 mL of triplex distilled water and 1.0 mL of 1% (v/v) $HAuCl_4$ solution were added into a round-bottom flask equipped with a reflux condenser under vigorous stirring. Then, the flask was incubated into an oil bath to reflux under stirring. When the solution was heated to a boiling state, 5.0 mL of 1% (v/v) trisodium citrate solution was quickly added to the flask, and then, the reaction was allowed to reflux for 20 min. The color of the solution changed from pale yellow to deep red, and the solution was cooled to room temperature and then stored at 4 °C in the refrigerator for further use.

Preparation of CdTe-Doped Silica Nanoparticles (CdTe@SiO_2). Prior to the preparation of CdTe-doped silica nanoparticles (CdTe@SiO_2), CdTe colloidal solutions were prepared. CdTe QDs were prepared using the reaction between Cd^{2+} and NaHTe solution at pH 8.30 with reduced glutathione (GSH) as the stabilizing reagent according to previous literature[29,30] with little modification. Generally, 0.057 g of $CdCl_2 \cdot 2.5H_2O$ and 0.192 g of GSH were dissolved in 100 mL of water under stirring conditions, and the pH value of the resulting solution was adjusted to 8.3 with l.0 M NaOH solution. After the solution was deaerated by bubbling N_2 for 30 min, 200 μL of 0.30 M oxygen-free NaHTe solution was immediately added to the solution, and then, the mixture solution was heated to 100 °C and refluxed in an oil bath for 4.5 h, and then, glutathione-capped CdTe QDs were obtained.

CdTe-doped silica nanoparticles were prepared with a revised Stöber method.[37,38] Typically, 20 mL of ethanol, 0.5 mL of CdTe aqueous solution, and 0.25 mL of TEOS were added into a round-neck flask and mixed under stirring. Then, 0.50 mL of 25% (m/m) $NH_3 \cdot H_2O$ was added, and the mixed solutions were allowed to react for 24 h under stirring. When the reaction was completed, the nanoparticles were isolated by acetone, followed by centrifuging and washing with ethanol and water for several cycles. Ultrasonication was performed while washing the nanoparticles to remove any physically absorbed molecules from the surface of nanoparticles.

Procedures for the Determination of Melamine. To investigate the energy transfer between CdTe@SiO_2 and AuNPs, the fluorescence intensities of the system of CdTe@SiO_2 mixed with

dx.doi.org/10.1021/jf300386y | J. Agric. Food Chem. 2012, 60, 4550−4558

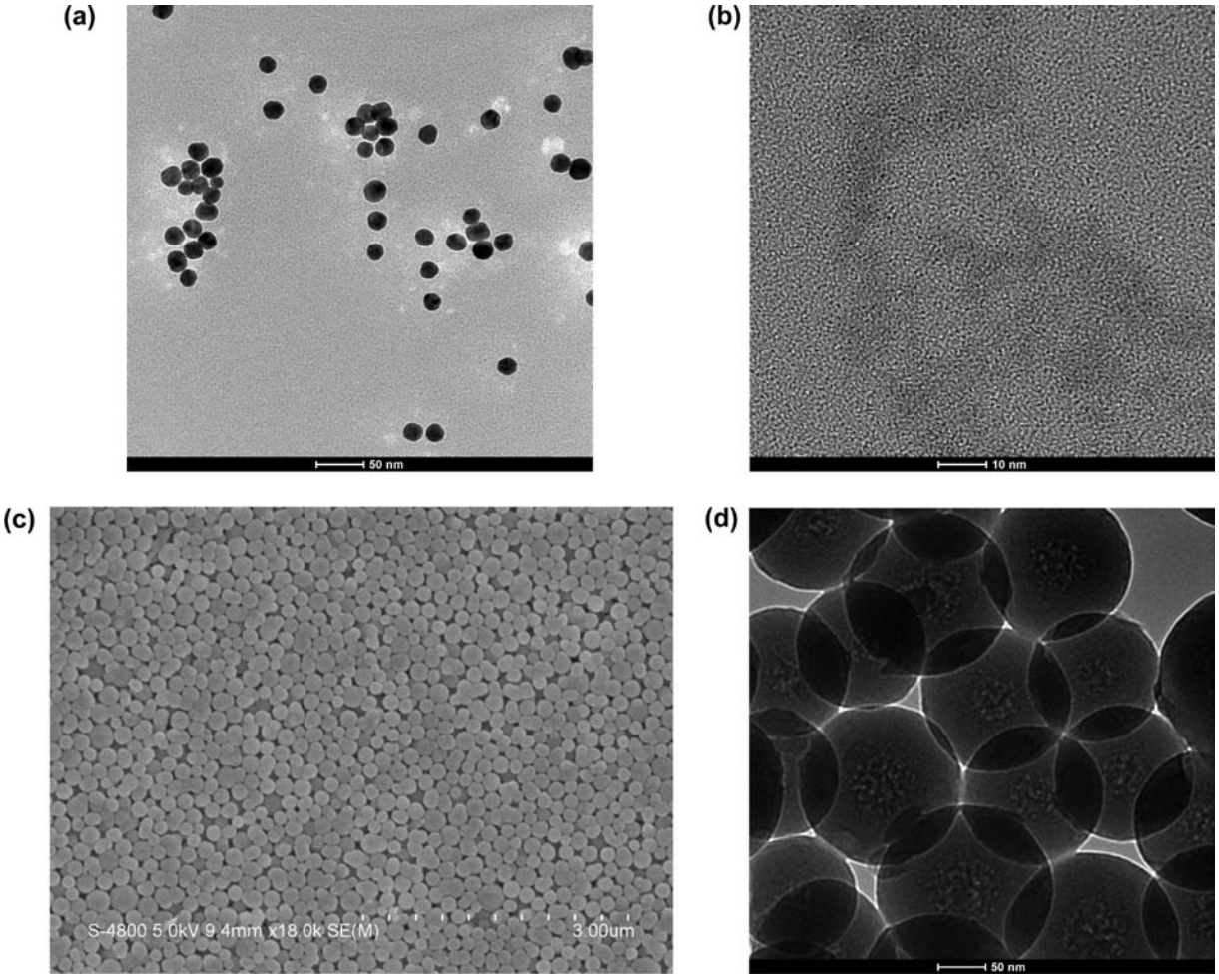

Figure 1. Typical TEM images of Au nanoparticles (A), CdTe QDs (B), and CdTe-doped silica nanoparticles (D) and SEM image of CdTe-doped silica nanoparticles (C).

different concentrations of AuNPs were recorded. Typically, 10 μL of CdTe@SiO_2 solution (40 mg mL^{-1}) and different aliquots of AuNPs were mixed and diluted to a final volume of 2.0 mL with 0.01 M phosphate buffer solution (pH 6.5), and then, the solution was equilibrated at ambient temperature for 30 min. The fluorescence intensities of the mixture solutions were measured at 561 nm with an excitation at 380 nm. The widths of excitation and emission slits were both set as 10 nm for the fluorescence measurements.

For the determination of melamine, 10 μL of CdTe@SiO_2 (40 mg mL^{-1}) and 7.0 mL of AuNPs (4.0 nM) and various amounts of melamine solution were mixed in a series of 10 mL volumetric flasks, and then, the mixture was diluted to the mark with pH 6.50 buffer solution and reacted thoroughly for 30 min at room temperature. The fluorescence intensities of the mixture solutions were measured at 561 nm with an excitation at 380 nm. The procedures for control experiments including FET between CdTe and AuNPs and the determination of melamine with CdTe−AuNPs system are the same as described above.

Prior to use, the real samples were treated with trichloroacetic acid to remove proteins. Typically, 5.0 mL of raw milk or 5.0 mg of milk powder was placed into a 10 mL centrifuge tube, and 1.5 mL of 2.0 M trichloroacetic acid was added and mixed with a vortex for 2 min to deposit protein in the sample matrix. The mixture was then centrifugated at 3500*g* for 5 min. The obtained supernatants were transferred into another centrifuge tube and adjusted to pH 7.0 with a small amount of 5 M NaOH and then were filtered with a 0.22 μm filter. One hundred microliters of the obtained filtrate was taken for recovery analysis.

RESULTS AND DISCUSSION

Morphological and Spectral Characterizations of AuNPs, CdTe QDs, and CdTe@SiO_2. Figure 1A displays the typical TEM images of the prepared AuNPs. It can be seen that the shapes of AuNPs are regular, monodisperse, and spherical, and the average size is about 13.1 ± 1.2 nm in diameter. Figure 2A shows the UV−vis absorption spectrum of AuNPs, and a characteristic surface plasmon resonance (SPR) peak located at 521 nm is observed.[27,28,40] The concentration of the AuNPs colloidal solution is estimated to be 4.0 nM according to Beer's law ($A = \varepsilon bc$). Herein, the extinction coefficient (ε) for 13 nm AuNPs at 521 nm is about 2.01×10^8 M^{-1} cm^{-1}.[27,28,40]

The typical TEM image of the prepared CdTe colloidal solution is displayed in Figure 1B. As shown in this figure, the shapes of CdTe QDs are regular and monodisperse, and the average size is about 2.7 ± 1.2 nm in diameter. Figure 2B displays the emission spectrum of CdTe QDs (curve a, black line), and it can be seen that the emission peak of CdTe is located at 575 nm under the excitation wavelength of 380 nm.

The SEM and TEM images of CdTe-doped silica nanoparticles (CdTe@SiO_2) prepared with a revised Stöber method are shown in Figure 1C,D, respectively. It can be seen that prepared CdTe@SiO_2 nanoparticles are uniform in size with a diameter of 150 nm. The nanoparticles can be dispersed very well in aqueous solutions, and the size can be controlled by

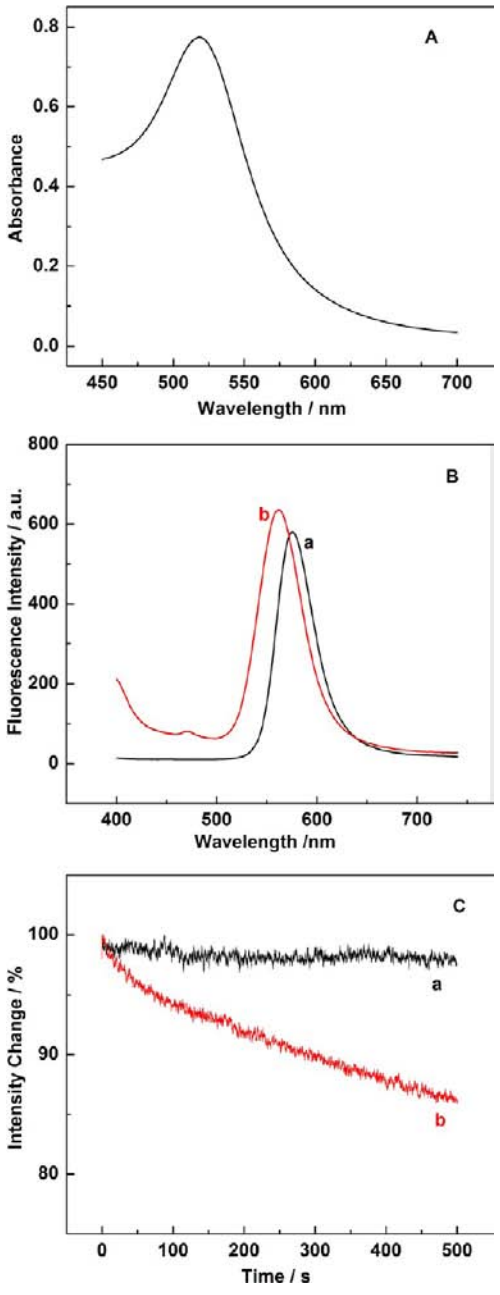

Figure 2. (A) Absorption spectrum of the prepared AuNPs, (B) fluorescence spectra of CdTe QDs (curve a, black line) and CdTe@SiO_2 nanoparticles (curve b, red line) under the same excitation of 380 nm, and (C) photobleaching experiments done on a spectrofluorometer of CdTe@SiO_2 (curve a, black line) and CdTe QDs (curve b, red line) with a 150 W xenon lamp excitation source. The concentrations for AuNPs, CdTe QDs, and CdTe@SiO_2 are 40 nM, 0.04 mg mL^{-1}, and 0.04 mg mL^{-1} in 0.01 M phosphate buffer (pH 6.50), respectively.

exchanging the ratio of TEOS and ammonium hydroxide when other parameters keep constant. Figure 2B (curve b, red line) displays the fluorescence spectra of CdTe@SiO_2 dispersion with the same excitation wavelength of 380 nm as for CdTe colloidal solution. As shown in this figure, the emission peak of CdTe@SiO_2 is located at 561 nm and has a little blue lift as compared with that of free CdTe. The blue shift of emission peak confirms the confinement of CdTe inside the silica cavity, which has less polarity as compared to bulk solution.[41] As we know, the emission peak of CdTe QDs depends on their size as a consequence of quantum confinement.[42] In this study, the synthesized CdTe@SiO_2 nanoparticles are expected as energy donors because its emission band at 561 nm could overlap with the adsorption band of energy acceptors AuNPs at 521 nm, as shown in Figure S1 in the Supporting Information.

To compare the photostability of CdTe@SiO_2 with that of free CdTe, the photobleaching experiments were carried out by investigating the variation of fluorescence intensity over a long period of continuous intensive excitation of 500 s with a 150 W xenon lamp. The results showed that there was almost no photobleaching for CdTe@SiO_2 over a long period of continuous intensive excitation of 500 s with a 150 W xenon lamp (Figure 2C, curve a). However, under the same experimental conditions, an obvious decrease in fluorescence intensity was observed for the free CdTe QDs ((Figure 2C, curve b). These experimental results indicate that the CdTe-doped silica nanoparticles possess good photostability and are suitable for the practical applications. The silica coatings isolate the CdTe QDs from the outside environment such as solvent molecules and free radicals caused by light exposure and, therefore, effectively prevent photodecomposition.[27,31−39]

Fluorescence Quenching Effect of AuNPs on CdTe@SiO_2. Figure 2A,B (curve b) show the absorption spectrum of AuNPs and fluorescence emission spectrum of CdTe@SiO_2 NPs, respectively. It can be seen that the emission spectra of CdTe@SiO_2 could overlap with the absorption spectra of AuNPs to an extent, as shown in Figure S1 in the Supporting Information, suggesting that FET between them can take place. According to FET process, in this system, CdTe@SiO_2 NPs act as donors, while AuNPs act as acceptors (quenchers).[23,24]

To further confirm the FET, we investigated the emission spectra of CdTe@SiO_2 in the presence of different concentrations of AuNPs. As shown in Figure 3A, the fluorescence intensities of CdTe@SiO_2 at a fixed concentration of 0.04 mg mL^{-1} were decreased gradually with the increasing of concentration of AuNPs ranging from 0.0 to 2.8 nM, and the maximum quenching was observed at the 2.8 nM AuNPs. This result indicates that when AuNPs were introduced into CdTe@SiO_2 solution, the energy was transferred from CdTe@SiO_2 to AuNPs, resulting in the quenching of the fluorescence intensity of CdTe@SiO_2. The quenching efficiency was calculated by $1 - I/I_0$, herein I_0 and I represent the fluorescence intensity of CdTe@SiO_2 in the absence (I_0) and presence (I) of AuNPs, respectively, and the maximum quenching efficiency of up to 90% was obtained when 2.8 nM AuNPs was introduced. This large quenching efficiency largely turns off the fluorescence of CdTe@SiO_2 and provides an optimal "off-state" for sensitive "turn-on" quantitative assay.

As shown in Figure 3B, the fluorescent intensity of CdTe@SiO_2−AuNPs system is inversely proportional to the concentration of AuNPs. The quenching constant (K_{sv}) was calculated according to the Stern−Volmer equation:[23]

$$I_0/I = K_{sv} \times [Q] + 1$$

Herein, I_0 and I represent the relative fluorescent intensity of CdTe@SiO_2 in the absence and presence of AuNPs, respectively, and [Q] is the concentration of the quencher (AuNPs). The plot of the relationship between I_0/I and [AuNPs] is shown in Figure 3B as an inset. It is clear that the plot is linear, and the Stern−Volmer equation can be fitted as:

$$I_0/I = 2.43[\text{AuNPs}]\ (\text{nM}) + 1 \quad (R = 0.9958)$$

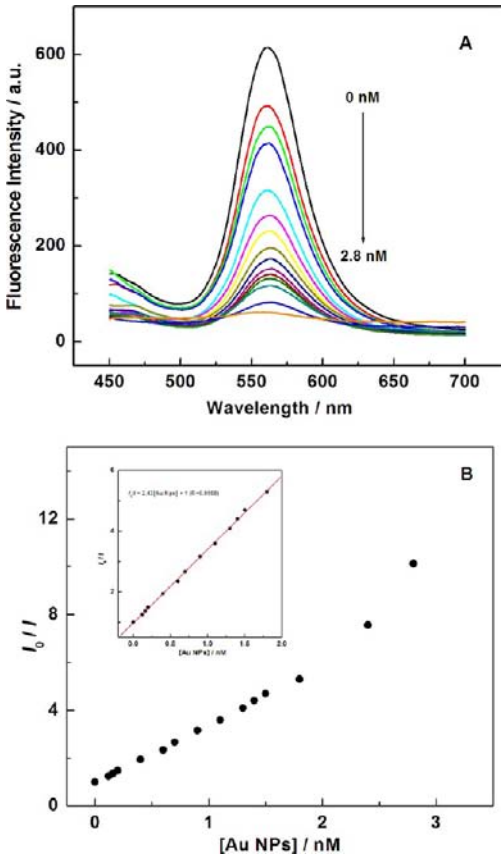

Figure 3. (A) Fluorescence spectra of CdTe@SiO_2 in the presence of various concentrations of AuNPs in 0.01 M phosphate buffer (pH 6.50). CdTe@SiO_2: 0.04 mg mL^{-1}; AuNPs (from top to bottom): 0, 0.04, 0.16, 0.2, 0.4, 0.6, 0.7, 0.9, 1.1, 1.3, 1.4, 1.5, 1.8, 2.4, and 2.8 nM. (B) Stern–Volmer plot of CdTe@SiO_2 nanoparticles quenched by AuNPs. The data are obtained from panel A.

From the slope of the linear plot, the quenching constant, K_{sv}, was found to be 2.43×10^9 M^{-1}. This large quenching constant suggests that AuNPs efficiently quench the fluorescence of CdTe@SiO_2 and are the proper energy acceptors for the donors CdTe@SiO_2 nanoparticles. The large quenching constant is also required to maximize the fluorescent changes and achieve an efficient "turn-on" detection of small amounts of analytes.

The fluorescence quenching of fluorophores by AuNPs is dominated by different mechanisms such as the inner filter effect,[43] photoinduced electron transfer,[44] and FET including fluorescence resonance energy transfer (FRET)[22,27,28] and surface energy transfer (SET).[45,46] In this study, the emission spectrum of CdTe@SiO_2 was overlapped with the absorption spectrum of AuNPs to a considerable extent, as shown in Figure S1 in the Supporting Information, and the locations of the maximum emission peaks of CdTe@SiO_2 did not show obvious changes in the presence of various concentrations of quenchers AuNPs, as shown in Figure 3A, suggesting that the fluorescence quench of CdTe@SiO_2 is more likely through energy transfer rather than electron transfer processes.[45,46] Such a FET process was also revealed in other systems with AuNPs as the energy acceptor.[45,46] A detailed mechanism investigation is right now in process in our lab.

For comparison, we also investigated the FET system between CdTe and AuNPs, in which CdTe as donors and AuNPs as acceptors. The emission spectra of CdTe colloidal solution varying with different concentrations of AuNPs are shown in Figure S2 in the Supporting Information. When the concentration of CdTe is fixed at 100 μM, the fluorescence intensities of free CdTe were decreased gradually with the increasing of concentrations of AuNPs ranging from 0.0 to 1.5 nM. The maximum quenching efficiency was calculated to be 71% when 1.5 nM AuNPs was introduced, which is lower than that of CdTe@SiO_2–AuNPs system (90%). The quenching constant (K_{sv}) was also calculated according to the Stern–Volmer equation. From the slope of the linear plot, the quenching constant, K_{sv}, was found to be 0.72×10^9 M^{-1}, which is also smaller than that of CdTe@SiO_2–AuNPs system (2.43×10^9 M^{-1}). These results demonstrate that the FET of CdTe@SiO_2–AuNPs system is more efficient than that of CdTe–AuNPs system. In the present system, the as-prepared AuNPs were capped with citrate ions and negatively charged at pH > 3.5,[28] while CdTe@SiO_2 nanoparticles were positively charged at pH < 7.0 due to the presence of protonated silanol groups (Si–OH_2^+) on the silica surface ($pK_a \sim 7.0$).[32] At pH 6.50, the AuNPs–CdTe@SiO_2 assemblies coalesce to form larger clusters, due to charge neutralization, resulting in the formation of CdTe@SiO_2–AuNPs compact assembly, which is favorable for AuNPs to harvest energy from CdTe doped in the SiO_2 shell. However, GSH-capped CdTe QDs are negatively charged at pH 6.5 because the isoelectronic point of GSH is 5.93.[47,48] So, in the CdTe–AuNPs system, the electronic repulsion reduces the energy transfer efficiency. In addition, we have demonstrated in our previous reports that the fluorophore-doped silica nanoparticles possess longer fluorescence lifetimes as compared with that of free fluorophore.[34,36] In the present system, CdTe@SiO_2 with prolonged fluorescence lifetime probably extends the energy transfer process to AuNPs, resulting in the enhanced energy transfer efficiency.

Fluorescence "Turn-On" Assay of Melamine. The effect of melamine on the FET system of CdTe@SiO_2–AuNPs has been investigated. Figure 4 depicts the emission spectra of CdTe@SiO_2, CdTe@SiO_2–melamine, CdTe@SiO_2–AuNPs, and CdTe@SiO_2–AuNPs–melamine under the same experimental conditions. As shown in this figure, CdTe@SiO_2 exhibits a strong fluorescent signal at about 561 nm (curve

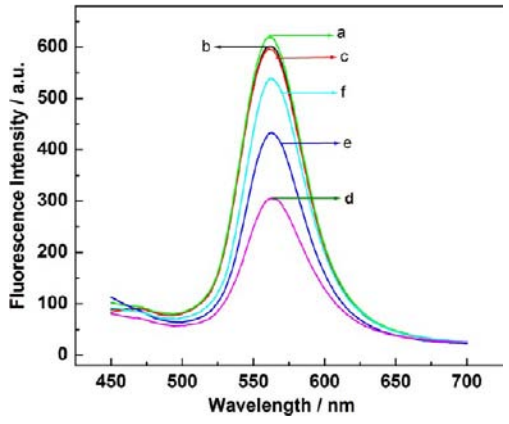

Figure 4. Fluorescence spectra of (a) 0.04 mg mL^{-1} CdTe@SiO_2, (b) a + 0.01 μM melamine, (c) a + 0.25 μM melamine, (d) a + 2.8 nM Au NPs, (e) a + 2.8 nM Au NPs + 0.01 μM melamine, and (f) a + 2.8 nM Au NPs + 0.25 μM melamine in 0.01 M phosphate buffer (pH 6.50).

dx.doi.org/10.1021/jf300386y | J. Agric. Food Chem. 2012, 60, 4550–4558

a), and its fluorescence intensity and peak location do not show obvious changes when 0.01 (curve b) and 0.25 μM (curve c) melamine were added to the solution, respectively, indicating that there were no obvious interaction between melamine and CdTe@SiO_2. When AuNPs was added into the CdTe@SiO_2 solution, the fluorescence intensity of CdTe@SiO_2 was decreased (curve d) due to the FET process between CdTe@SiO_2 and AuNPs. When 0.01 (curve e) and 0.25 μM (curve f) melamine was added into the CdTe@SiO_2–AuNPs mixture solution, respectively, the fluorescence of CdTe@SiO_2–AuNPs system was restored, suggesting that AuNPs released from the surfaces of CdTe@SiO_2 due to the binding of melamine to AuNPs through Au–N bond. On the basis of the restored fluorescence, a fluorescent "turn-on" method for the determination of melamine was proposed.

Optimization of Experimental Conditions for the Detection of Melamine. The parameters including media pH, incubation time, and AuNPs concentration were optimized for the CdTe@SiO_2–AuNPs system and the detection of melamine. In this study, the selection of media pH was based on two aspects. On one hand, in the present system, the interaction between amino group and AuNPs is critical for the determination of melamine. As reported in the literature, media pH affects the interaction of AuNPs with a small molecule. Melamine is a weak base with a pK_a of 9.0,[1] and media pH also affects the form of melamine in aqueous solution. In strong acidic media or strong basic media, melamine can be hydrolyzed, and amino groups could be gradually lost, finally transforming into cyanuric acid, which could not interact with AuNPs.[19] On the other hand, as described above, the as-prepared AuNPs were capped with citrate ions and negatively charged at pH > 3.5, while CdTe@SiO_2 nanoparticles were positively charged at pH <7.0. To form compact CdTe@SiO_2–AuNPs assembly via electrostatic attraction interaction, and as such to obtain more efficient energy transfer, a weak acid medium is required. Taking the above two points into consideration, pH 6.5 was recommended and used throughout in this study.

At room temperature, the time dependence of the reaction between the CdTe@SiO_2–AuNPs system and the melamine was investigated, and the result reveals that the maximal enhanced fluorescence signal was achieved within ca. 30 min of incubation and then kept stable. To ensure complete fluorescence recovery and obtain stable signal, 30 min of incubation was recommended in this step.

In the construction of FET systems, it is of great importance to find energy acceptors with as large as possible power to quench the emission of donors. Generally, a larger quenching efficiency will lead to higher detection sensitivity in "turn-on" quantitative assays. As described above, in the present FET system, the maximum quenching efficiency was observed when 2.8 nM AuNPs was introduced into a fixed CdTe@SiO_2 concentration of 0.04 mg mL^{-1}. For the above reason, 2.8 nM AuNPs was chosen as the optimum concentration in the FET system for the following detection of melamine.

Detection of Melamine. Under the optimum experimental conditions, the analytical parameters for the determination of melamine were evaluated. Figure 5A displays the fluorescence spectra of the CdTe@SiO_2–AuNPs FET system in the presence of varying concentrations of melamine. As shown in this figure, with increasing the concentration of melamine, the fluorescence intensity of CdTe@SiO_2–AuNPs is increased gradually. The plot of the fluorescence enhanced efficiency,

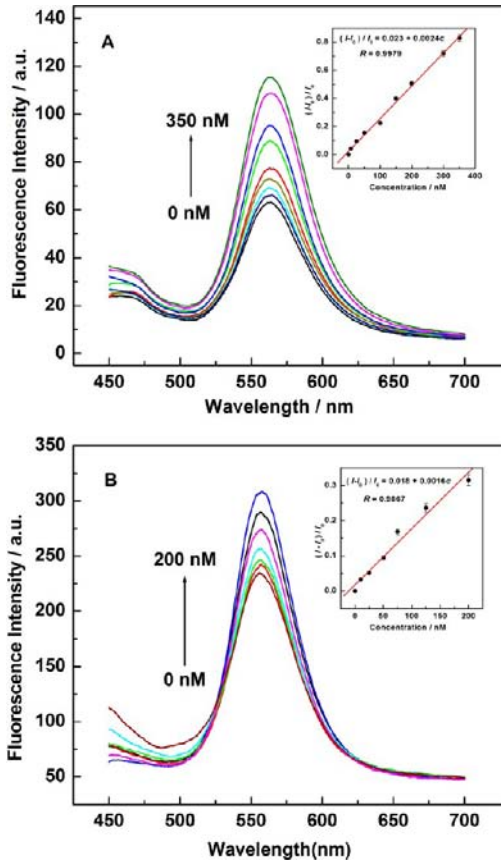

Figure 5. (A) Fluorescence spectra of the CdTe@SiO_2–AuNPs system in the presence of different concentrations of melamine in 0.01 M phosphate buffer (pH 6.50). From bottom to top: 0, 7.5×10^{-9}, 2.5×10^{-8}, 5×10^{-8}, 1×10^{-7}, 1.5×10^{-7}, 2×10^{-7}, 3×10^{-7}, and 3.5×10^{-7} M. CdTe@SiO_2, 0.04 mg mL^{-1}; Au NPs, 2.8 nM. Inset: the enhanced fluorescence intensities as a function of concentration of melamine. (B) Fluorescence spectra of the CdTe–AuNPs system in the presence of different concentrations of melamine. From bottom to top: 0, 1×10^{-8}, 2.5×10^{-8}, 5×10^{-8}, 7.5×10^{-8}, 1.25×10^{-7}, and 2×10^{-7} M. CdTe, 100 μM; AuNPs, 1.5 nM. Inset: the enhanced fluorescence intensities as a function of the concentration of melamine.

which is defined as $(I - I_0)/I_0$, and I and I_0 represent the fluorescence intensity in the presence of different concentrations of melamine and the absence of melamine, respectively, against the concentration of added melamine, which is also shown in Figure 5A as an inset. It is clear that the fluorescence-enhanced efficiency exhibits a linear response to the melamine concentration in the range of $7.5 \times 10^{-9} \sim 3.5 \times 10^{-7}$ M (i.e., 1.0–44 ppb) with a correlation coefficient of 0.9979, and the calibration curve can be expressed as $(I - I_0)/I_0 = 0.023 + 0.0024c$ (c: nM). The limit of detection ($3\sigma/s$) for melamine is 8.9×10^{-10} M (i.e., 0.11 ppb). Where σ represents the standard deviation of eight blank measurements, and s is the slope of calibration curve. These analytical parameters are better or favorably comparable to those reported in the literature, as shown in Table 1. The repeatability of the proposed methods was also evaluated by measurements of 5.0×10^{-8} M melamine, and the relative standard deviation for seven repeated measurements was found to be 4.37%, indicating that the response of the CdTe@SiO_2–AuNPs to melamine is highly reproducible.

For comparison, a control experiment using the FET system between CdTe and AuNPs to detect melamine was also

dx.doi.org/10.1021/jf300386y | J. Agric. Food Chem. 2012, 60, 4550–4558

Table 1. Comparison of Analytical Parameters of Different Methods for the Determination of Melamine

methods	linear range (μM)	detection limit (μM)	ref.
reversed phase high-performance liquid chromatography	7.93−634	0.793	3
reversed phase high-performance liquid chromatography coupled with diode array detection	0.793−396	0.793	4
high-performance liquid chromatography−triple-quadrupole mass spectrometry (HPLC-MS/MS)		0.238	5
gas chromatography/mass spectrometry (GC/MS)	0.396−1.59	0.0793	6
gas chromatography−mass spectrometric (GC-MS) method	0.396−0.793	0.0396	7
high-performance liquid chromatography/tandem mass spectrometry (HPLC/MS/MS)	0.396−79.29		8
direct analysis in real time ion source coupled to time-of-flight mass spectrometry (TOFMS)		1.35	10
high-performance micellar electrokinetic capillary chromatography with amperometric detection	0.794−0.0159	0.0167	11
capillary zone electrophoresis with diode array detection	0.396−79.3	0.0792	12
ELISA	0.00006−0.0058	0.0206	13
single-run electrochemical method	5−200	8.0	15
electrochemical sensor for melamine based on its copper complex	0.01−0.15	0.002	16
colorimetric method/AuNPs	1.59−79.3	0.476	19
colorimetric method/AuNPs	0.001−10	0.0008	20
fluorimetry method with cucurbit[7]uril as probe	0.6−200	1.59	21
FRET/fluorescein-AuNPs	0.1−4.0	0.001	22
microfluidic electrophoresis device coupled with ultraviolet detection	7.94−794	1.83	49
FRET/CdTe@SiO2-AuNPs	0.0075−0.35	0.89	this work

Table 2. Results of the Determination of Melamine in Real Samples[a]

		nM/ppb		
samples	original	spiked	found	recovery %
milk powder				
		25.0/3.2	25.2 ± 0.1/3.2 ± 0.0	100.7 ± 0.1
		100.0/12.8	102.3 ± 0.5/12.9 ± 0.1	102.3 ± 0.5
		200.0/25.6	197.6 ± 0.8/24.9 ± 0.1	99.8 ± 0.4
raw milk				
		25.0/3.2	24.3 ± 0.7/3.1 ± 0.1	97.4 ± 0.0
		100.0/12.8	101.1 ± 0.4/12.7 ± 0.1	101.1 ± 0.4
		200.0/25.6	209.0 ± 1.2/26.4 ± 0.2	104.1 ± 0.6

[a]Average of five repeated measurements.

performed. The procedures for the detection of melamine are similar to that for CdTe@SiO_2−AuNPs system. The fluorescence spectra of the CdTe−AuNPs system with different concentrations of melamine are shown in Figure 5B, and the plot of the fluorescence enhanced efficiency versus the concentration of added melamine is also shown in Figure 5B as an inset. The calibration equation is $(I - I_0)/I_0 = 0.018 + 0.0016c$ (c: nM) in the range from 1×10^{-8} to 2×10^{-7} M (i.e., 1.3−25.0 ppb) with a correlation coefficient of 0.9867. It is clear that the sensitivity of CdTe@SiO_2−AuNPs system to melamine (i.e., the ratio of slopes of regression equation for these two probe systems) is 50% higher than that of CdTe−AuNPs system. The detection limit was also calculated to be 5.3×10^{-9} M (i.e., 0.67 ppb), which is 5.0-fold higher than that of CdTe@SiO_2−AuNPs system. The repeatability of the CdTe−AuNPs probe system was also evaluated by measurements of 5.0×10^{-8} M melamine, and the relative standard deviation for seven repeated measurements was found to be 10%, suggesting that CdTe@SiO_2−AuNPs system to melamine is more reproducible than the CdTe−AuNPs system. These improved analytical performances could be attributed to the excellent photostability of CdTe-doped silica nanoparticles and the enhanced FET between CdTe@SiO_2 and AuNPs.

Effect of Potential Interfering Substances. To determine melamine in real samples such as raw milk and milk powder, the potential interfering substances including common ions, amino acids, and some organic molecules were investigated to evaluate the selectivity of the proposed method. To evaluate the selectivity, we investigated the fluorescence response of CdTe@SiO_2−AuNPs system to melamine at a concentration of 100 nM (1.26×10^{-7} g L^{-1}) in the presence of different interfering substances. The effects of main relevant metal ions such as K^+, Na^+, Mg^{2+}, Zn^{2+}, Fe^{2+}, Fe^{3+}, Cl^-, NO_3^-, and SO_4^{2-} on the fluorescence intensity of the present system for 100 nM melamine were studied, and the results showed that the 10000-fold excesses of Na^+ and K^+, 1000-fold excesses of Mg^{2+} and Zn^{2+}, 700-fold excesses of Fe^{2+}, and 400-fold excesses of Fe^{3+} induced less than ±5% interference with the detection of the melamine. The common species in raw milk, such as Ca^{2+}, urea, vitamin B, and vitamin C with the content of 370, 300, 200, and 20 mg kg^{-1},[19] respectively, did not show interference in the determination of 100 nM melamine. Because the amino group (NH_2−) in amino acids can interact with AuNPs, amino acids and some proteins can also enhance the fluorescence of the CdTe@SiO_2−AuNPs system. Combined with proper pretreatment or separation technology, it is promising to apply this method to detect melamine in milk products. These results suggested that the CdTe@SiO_2−AuNPs system possessed a good selective fluorescence response toward melamine and also indicated that a "turn-on" fluorescent method for the determination of melamine could be developed by the present system.

Analysis of Melamine in Real Samples. To validate the proposed method to specifically detect melamine in real

samples, the amounts of melamine in commercial in raw milk and milk powder were measured by standard addition method under the optimized conditions. Certain amounts of melamine standard solution were directly spiked into the real samples because the existing milk products in the market are free of melamine. The results of real samples by standard addition method are summarized in Table 2. As shown in Table 2, excellent recoveries in the range from 97 to 104% were obtained for all samples, suggesting that the proposed method is reliable and suitable for real applications.

In summary, we here developed an efficient and enhanced FET system between confined CdTe (CdTe@SiO_2) as donors and AuNPs as acceptors. The enhanced quenching effect largely turns off the fluorescence of CdTe@SiO_2 and provides an optimal "off-state" for sensitive "turn-on" assay of melamine. The proposed method displays high sensitivity and a low limit of detection for the determination of melamine and can be applied to the determination of melamine in real samples with satisfactory recoveries. Such a FET system between confined QDs and AuNPs may pave a new way for designing chemo/biosensing. However, some further investigations including detailed mechanisms of FET and the effect of the sizes of CdTe@SiO_2 and AuNPs on the energy transfer are required and currently in process in our lab.

■ ASSOCIATED CONTENT

Ⓢ Supporting Information

Figures of emission and adsorption spectra, fluorescence spectra, and plot of the I_0/I as a function of the concentration of AuNPs. This material is available free of charge via the Internet at http://pubs.acs.org.

■ AUTHOR INFORMATION

Corresponding Author

*Tel: +86-553-3937136. Fax: +86-553-3869302. E-mail: fgao@mail.ahnu.edu.cn.

Funding

We are grateful for the financial support from the Natural Science Foundation of China (Grant Nos. 21175002 and 21055001) and Anhui Provincial Natural Science Foundation for Distinguished Youth (Grant No. 1108085J09).

Notes

The authors declare no competing financial interest.

■ REFERENCES

(1) Bann, B.; Samuel A. Miller, S. A. Melamine and derivatives of melamine. *Chem. Rev.* **1958**, *58*, 131−172.

(2) Lam, C. W.; Lan, L.; Che, X.; Tam, S.; Wong, S.; Chen, Y.; Jin, J.; Tao, S. H.; Tang, X. M.; Yuen, K. Y.; Tam, P. K. Diagnosis and spectrum of melamine-related renal disease: Plausible mechanism of stone formation in humans. *Clin. Chim. Acta* **2009**, *402*, 150−155.

(3) Venkatasami, G.; Sowa, J. R., Jr. A rapid, acetonitrile-free, HPLC method for determination of melamine in infant formula. *Anal. Chim. Acta* **2010**, *665*, 227−230.

(4) Sun, H.; Wang, L.; Ai, L.; Liang, S.; Wu, H. A sensitive and validated method for determination of melamine residue in liquid milk by reversed phase high-performance liquid chromatography with solid-phase extraction. *Food Control* **2010**, *21*, 686−691.

(5) Tran, B. N.; Okoniewski, R.; Storm, R.; Jansing, R.; Aldous, K. M. Use of methanol for the efficient extraction and analysis of melamine and cyanuric acid residues in dairy products and pet foods. *J. Agric. Food Chem.* **2010**, *58*, 101−107.

(6) Xu, X. M.; Ren, Y. P.; Zhu, Y.; Cai, Z. X.; Han, J. L.; Huang, B. F.; Zhu, Y. Direct determination of melamine in dairy products by gas chromatography/mass spectrometry with coupled column separation. *Anal. Chim. Acta* **2009**, *650*, 39−43.

(7) Zhu, X.; Wang, S.; Liu, Q.; Xu, Q.; Xu, S.; Chen, H. Determination of residues of cyromazine and its metabolite, melamine, in animal-derived food by gas chromatography-mass spectrometry with derivatization. *J. Agric. Food Chem.* **2009**, *57*, 11075−11080.

(8) Filigenzi, M. S.; Puschner, B.; Aston, L. S.; Poppenga, R. H. Diagnostic determination of melamine and related compounds in kidney tissue by liquid chromatography/tandem mass spectrometry. *J. Agric. Food Chem.* **2008**, *56*, 7593−7599.

(9) Yokley, R. A.; Mayer, L. C.; Rezaaiyan, R.; Manuli, M. E.; Cheung, M. W. Analytical method for the determination of cyromazine and melamine residues in soil using LC-UV and GC-MSD. *J. Agric. Food Chem.* **2000**, *48*, 3352−3358.

(10) Vaclavik, L.; Rosmus, J.; Popping, B.; Hajslova, J. Rapid determination of melamine and cyanuric acid in milk powder using direct analysis in real time-time-of-flight mass spectrometry. *J. Chromatogr. A* **2010**, *1217*, 4204−4211.

(11) Wang, J. Y.; Jiang, L. M.; Chu, Q. C.; Ye, J. N. Residue analysis of melamine in milk products by micellar electrokinetic capillary chromatography with amperometric detection. *Food Chem.* **2010**, *121*, 215−219.

(12) Yan, N.; Zhou, L.; Zhu, Z.; Chen, X. Determination of melamine in dairy products, fish feed, and fish by capillary zone electrophoresis with diode array detection. *J. Agric. Food Chem.* **2009**, *57*, 807−811.

(13) Lei, H. T.; Shen, Y. D.; Song, L. J.; Yang, J.; Chevallier, O. P.; Haughey, S. A.; Wang, H.; Sun, Y.; Elliott, C. Hapten synthesis and antibody production for the development of a melamine immunoassay. *Anal. Chim. Acta* **2010**, *665*, 84−90.

(14) Fodey, T. L.; Thompson, C. S.; Traynor, I. M.; Haughey, S. A.; Kennedy, D.G..; Crooks, S. R. H. Development of an optical biosensor based immunoassay to screen infant formula milk samples for adulteration with melamine. *Anal. Chem.* **2011**, *83*, 5012−5016.

(15) Liao, C. W.; Chen, Y. R.; Chang, J. L.; Zen, J. M. Single-run electrochemical determination of melamine in dairy products and pet foods. *J. Agric. Food Chem.* **2011**, *59*, 9782−9787.

(16) Zhu, H.; Zhang, S.; Li, M.; Shao, Y.; Zhu, Z. Electrochemical sensor for melamine based on its copper complex. *Chem. Commun.* **2010**, *46*, 2259−2261.

(17) Yu, J.; Zhang, C.; Dai, P.; Ge, S. Highly selective molecular recognition and high throughput detection of melamine based on molecularly imprinted sol-gel film. *Anal. Chim. Acta* **2009**, *651*, 209−214.

(18) Zeng, H. J.; Yang, R.; Wang, Q. W.; Li, J. J.; Qu, L. B. Determination of melamine by flow injection analysis based on chemiluminescence system. *Food Chem.* **2011**, *127*, 842−846.

(19) Li, L.; Li, B.; Cheng, D.; Mao, L. Visual detection of melamine in raw milk using gold nanoparticles as colorimetric probe. *Food Chem.* **2010**, *122*, 895−900.

(20) Cao, Q.; Zhao, H.; He, Y.; Li, X.; Zeng, L.; Ding, N.; Wang, J.; Yang, J.; Wang, G. Hydrogen-bonding-induced colorimetric detection of melamine by nonaggregation-based Au-NPs as a probe. *Biosens. Bioelectron.* **2010**, *25*, 2680−2685.

(21) Zhou, Y. Y.; Yang, J.; Liu, M.; Wang, S. F.; Lu, Q. A novel fluorometric determination of melamine using cucurbit[7]uril. *J. Lumin.* **2010**, *130*, 817−820.

(22) Guo, L.; Zhong, J.; Wu, J.; Fu, F.; Chen, G.; Chen, Y.; Zheng, X.; Lin, S. Sensitive turn-on fluorescent detection of melamine based on fluorescence resonance energy transfer. *Analyst* **2011**, *136*, 1659−1663.

(23) Lakowicz, J. R. *Principles of Fluorescence Spectroscopy*, 3rd ed.; Springer-Verlag: Berlin Heidelberg, Berlin, 2006.

(24) Sapsford, K. E.; Berti, L.; Medintz, I. L. Materials for fluorescence resonance energy transfer analysis: Beyond traditional donor-acceptor combinations. *Angew. Chem., Int. Ed.* **2006**, *45*, 4562−4588.

(25) Link, S.; El-Sayed, M. A. Spectral properties and relaxation dynamics of surface plasmon electronic oscillations in gold and silver nanodots and nanorods. *J. Phys. Chem. B* **1999**, *103*, 8410−8426.
(26) Thomas, K. G.; Kamat, P. V. Chromophore-functionalized gold nanoparticles. *Acc. Chem. Res.* **2003**, *36*, 888−898.
(27) Gao, F.; Cui, P.; Chen, X.; Ye, Q.; Li, M.; Wang, L. A DNA hybridization detection based on fluorescence resonance energy transfer between dye-doped core-shell silica nanoparticles and gold nanoparticles. *Analyst* **2011**, *136*, 3973−3980.
(28) Gao, F.; Ye, Q.; Cui, P.; Chen, X.; Li, M.; Wang, L. Selective "turn-on" fluorescent sensing for biothiols based on fluorescence resonance energy transfer between acridine orange and gold nanoparticles. *Anal. Methods* **2011**, *3*, 1180−1185.
(29) Xue, M.; Wang, X.; Wang, H.; Chen, D.; Tang, B. Hydrogen bond breakage by Fluoride anion in a simple CdTe quantum dot/Gold nanoparticle FRET system and its analytical application. *Chem. Commun.* **2011**, *47*, 4986−4988.
(30) Tang, B.; Cao, L.; Xu, K.; Zhuo, L.; Ge, J.; Li, Q.; Yu, L. A new nanobiosensor for glucose with high sensitivity and selectivity in serum based on fluorescence resonance energy transfer (FRET) between CdTe quantum dots and Au nanoparticles. *Chem.—Eur. J.* **2008**, *14*, 3637−3644.
(31) Santra, S. M.; Zhang, P.; Wang, K.; Tapec, R.; Tan, W. Conjugation of biomolecules with luminophore-doped silica nanoparticles for photostable biomarkers. *Anal. Chem.* **2001**, *73*, 4988−4993.
(32) Santra, S.; Yang, H.; Dutta, D.; Stanley, J. T.; Holloway, P. H.; Tan, W.; Moudgil, B. M.; Mericle, R. A. TAT conjugated, FITC doped silica nanoparticles for bioimaging applications. *Chem.Commun.* **2004**, 2810−2811.
(33) Luo, F. B.; Yin, J.; Gao, F.; Wang, L. A non-enzyme hydrogen peroxide sensor based on core/shell silica nanoparticles using synchronous fluorescence spectroscopy. *Microchim. Acta* **2009**, *165*, 23−28.
(34) Gao, F.; Luo, F. B.; Yin, J.; Wang, L. Preparation of aminated core-shell fluorescent nanoparticles and its application to the synchronous fluorescence determination of γ-Globulin. *Luminescence* **2008**, *23*, 392−396.
(35) Gao, F.; Wang, L.; Tang, L.; Zhu, C. A novel nano-sensor based on rhodamine-β-isothiocyanate-doped silica nanoparticle for pH measurement. *Microchim. Acta* **2005**, *152*, 131−135.
(36) Gao, F.; Chen, X.; Ye, Q.; Yao, Z.; Guo, X.; Wang, L. Core-shell fluorescent silica nanoparticles for sensing near-neutral pH values. *Microchim. Acta* **2011**, *172*, 327−333.
(37) Gao, F.; Luo, F.; Chen, X.; Yao, W.; Yin, J.; Yao, Z.; Wang, L. A novel nonenzymatic fluorescent sensor for glucose based on silica nanoparticles doped with europium coordination compound. *Talanta* **2009**, *80*, 202−206.
(38) Nann, T.; Mulvaney, P. Single quantum dots in spherical silica particles. *Angew. Chem., Int. Ed.* **2004**, *43*, 5393−5396.
(39) Gao, F.; Tang, L.; Dai, L.; Wang, L. A fluorescence ratiometric nano-pH sensor based on dual-fluorophore-doped silica nanoparticles. *Spectrochim. Acta, Part A* **2007**, *67*, 517−521.
(40) Lim, I. S.; Gorolesk, F.; Mott, D.; Kariuki, N.; Ip, W.; Luo, J.; C. Zhong, C. Adsorption of cyanine dyes on gold nanoparticles and formation of j-aggregates in the nanoparticle assembly. *J. Phys. Chem. B* **2006**, *110*, 6673−6682.
(41) Yang, Y. H.; Gao, M. Y. Preparation of fluorescent SiO_2 particles with single CdTe nanocrystal cores by the reverse microemulsion method. *Adv. Mater.* **2005**, *17*, 2354−2357.
(42) Wang, Z.; Li, J.; Liu, B.; Hu, J.; Yao, X.; Li, J. Chemiluminescence of CdTe nanocrystals induced by direct chemical oxidation and its size-dependent and surfactant-sensitized effect. *J. Phys. Chem. B* **2005**, *109*, 23304−23311.
(43) Lim, S. Y.; Kim, J. H.; Lee, J. S.; Park, C. B. Gold nanoparticle enlargement coupled with fluorescence quenching for highly sensitive detection of analytes. *Langmuir* **2009**, *25*, 13302−13305.
(44) Shang, L.; Yin, J.; Li, J.; Jin, L.; Dong, S. Gold nanoparticles-based near-infrared fluorescent detection of biological thiols in human plasma. *Biosens. Bioelectron.* **2009**, *25*, 269−274.
(45) Sen, T.; Jana, S.; Koner, S.; Patra, A. Energy transfer between confined dye and surface attached Au nanoparticles of mesoporous silica. *J. Phys. Chem. C* **2010**, *114*, 707−714.
(46) Yun, C. S.; Javier, A.; Jennings, T.; Fisher, M.; Hira, S.; Peterson, S.; Hopkins, B.; Reich, N. O.; Strouse, G. F. Nanometal surface energy transfer in optical rulers, breaking the FRET barrier. *J. Am. Chem. Soc.* **2005**, *127*, 3115−3119.
(47) Zheng, Y.; Gao, S.; Ying, J. Y. Synthesis and cell-imaging applications of glutathione-capped CdTe quantum dots. *Adv. Mater.* **2007**, *19*, 376−380.
(48) Gao, M.; Cao, C.; Liu, M.; Wang, P.; Zhu, C. Selective fluorometry of cytochrome C using glutathione-capped CdTe quantum dots in weakly basic medium. *Microchim. Acta* **2009**, *165*, 341−346.
(49) Zhai, C.; Qiang, W.; Sheng, J.; Lei, J.; Ju, H. Pretreatment-free fast ultraviolet detection of melamine in milk products with a disposable microfluidic device. *J. Chromatogr., A* **2010**, *1217*, 785−789.